The Astrophysical Journal, 696:1972–1980, 2009 May 10 doi:10.1088/0004-637X/696/2/1972


# INFLUENCE OF DOPPLER WIDTH FLUCTUATIONS ON THE SHAPE OF SPECTRAL LINES

N. A. Silant'ev[1], E. E. Lekht[1,2], and G. A. Alexeeva[3]
[1] Instituto Nacional de Astrofísica, Óptica y Electrónica, Apartado Postal 51 y 216, 72840, Tonantzintla, Puebla, México; silant@inaoep.mx
[2] Sternberg Astronomical Institute, 13 Universitetskij prospect, Moscow, 119992, Russia
[3] Central (Pulkovo) Astronomical Observatory of Russian Academy of Sciences, Pulkovskoe shosse 65, St. Petersburg, 196140, Russia
*Received 2008 October 2; accepted 2009 February 20; published 2009 April 28*

## ABSTRACT

We investigate the influence of stochastic Doppler width fluctuations on the shape of spectral lines. The photospheres and atmospheres of stars, and the interstellar medium, possess stochastic behavior especially near nonstationary objects such as active galactic nuclei, quasars, flare stars, and regions of star formation. In reality, we observe the mean values of intensities from these objects. In most situations, the spectral line extinction coefficient has a Gaussian shape with the stochastic Doppler width determined by thermal and small-scale turbulent motions of atoms or molecules. For small-scale turbulent motions (short-correlated turbulence) the propagation of radiation is described by the average extinction factor. This coefficient depends on the level of the Doppler width fluctuations $\eta$. We show that these fluctuations change both the value of intensity and the shape of spectral lines. We consider distortions of the spectral line shapes for the absorption and emission lines for various values of the parameter $\eta$. For a number of $H_2O$ maser sources we estimate the values of this parameter, the optical depths of the inverted media, and the mean effective Doppler velocities. Maser emission lines with non-Gaussian shape can serve as an additional method for the investigation of the physical parameters in maser "spots."

*Key words:* masers – radiative transfer – stars: atmospheres – turbulence

## 1. INTRODUCTION

Many photospheres and atmospheres of stars have chaotic (turbulent) motions of gas (see, for example, Gray 1992; Sobolev 1969), especially in such nonstationary objects as variable and flare stars (Gurzadyan 1980; Sterken & Jaschek 1996). The motions and temperature of interstellar matter near active galactic nuclei, quasars, and regions of stellar formation are also stochastic. In turbulent (more generally, stochastic) media, the extinction coefficient $\alpha_\nu$, the intensity of radiation $I_\nu$, the temperature $T$, etc., are also the stochastic values. They are characterized by their mean values, $\alpha_\nu^{(0)}$, $I_\nu^{(0)}$, $T^{(0)}$, and by the fluctuating components, $\alpha_\nu'$, $I_\nu'$, $T'$. So we have $\alpha_\nu = \alpha_\nu^{(0)} + \alpha_\nu'$, $I_\nu = I_\nu^{(0)} + I_\nu'$, $T = T^{(0)} + T'$ etc., where the mean values of the fluctuating quantities are equal to zero, for example, $\langle T' \rangle = 0$.

Usually, the observed radiation intensity is collected from many volumes with different temperatures and small-scale turbulent velocities. In reality, we observe the mean intensity $I^{(0)}$ corresponding to many realizations of conditions in cosmic sources (for more details, see Levshakov & Kegel 1997). For a small-scale turbulent medium, the mean intensity $I^{(0)}$ obeys the usual transfer equation with an average extinction factor $\alpha_\nu^{(0)}$ (see Silant'ev 2005; Silant'ev et al. 2006). This coefficient depends on both the mean temperature $T^{(0)}$, mean turbulent velocity $u_{\rm turb} = \langle u(\mathbf{r}, t) \rangle$, etc., and the levels of the corresponding fluctuating values. So the value $\alpha_\nu^{(0)}$ differs from the usual extinction factor taken at the mean temperature $T^{(0)}$, mean turbulent velocity $u_{\rm turb}$, etc. This implies that the observed mean intensity $I_\nu^{(0)}$ acquires another value and spectral form than those in the media without the stochastic fluctuations.

The distortion of spectra in a continuum was considered by Silant'ev & Alexeeva (2008). Here, we consider the change of spectral line shape due to existence of temperature fluctuations and fluctuations of small-scale turbulent velocity $u_{\rm turb}$. In most cases, one observes spectral lines with Doppler widths $\Delta\nu_D$. We consider here only this case. As is known, the Doppler width is described by the expression

$$\Delta\nu_D = \frac{\nu_0}{c}\sqrt{\frac{2}{3}}\sqrt{u_{th}^2 + u_{\rm turb}^2} \equiv \frac{\nu_0}{c}\sqrt{\frac{2}{3}}u_D, \qquad u_D = \sqrt{u_{th}^2 + u_{\rm turb}^2}, \tag{1}$$

where $u_{th}^2 = 3kT/m$ and $u_{\rm turb}^2 = \langle u^2(\mathbf{r}, t) \rangle$ are the squares of the rms values of thermal and small-scale turbulent velocities, respectively, $u_D$ is the effective 3D Doppler velocity, $\nu_0$ is the central frequency of the spectral line, $c$ is the light velocity, and $k$ is the Boltzmann constant. Remember that the temperature and velocity $u_{\rm turb}$ are different in different observed volumes, i.e., they can be considered as stochastic values. As a result, the Doppler width is also stochastic and characterized by its mean value and the fluctuating part

$$\Delta\nu_D = \Delta\nu_D^{(0)} + \Delta\nu_D'. \tag{2}$$

The level of the Doppler width fluctuations is defined by the expression

$$\eta = \frac{\sqrt{\langle (\Delta\nu_D')^2 \rangle}}{\Delta\nu_D^{(0)}}. \tag{3}$$

The extinction coefficient with the Doppler width has the form (see, for example, Rybicki & Lightman 1979)

$$\alpha_\nu = \frac{\alpha_0}{\Delta\nu_D}\exp\left[-\left(\frac{\nu - \nu_0}{\Delta\nu_D}\right)^2\right]. \tag{4}$$

Without any restriction we omitted here the regular velocity of the source which determines the central position of the line. The value $\alpha_0$ is proportional to the quantum mechanical cross-section $\sigma_0$ at the center of the line. The more general expression for the $\alpha_\nu$-coefficient (the Voigt formula) is discussed by Hummer (1962). This expression represents the Doppler and the Lorentz line shapes as limiting cases.

## 2. QUALITATIVE EXPLANATION OF STOCHASTIC EFFECTS

To demonstrate qualitatively how the Doppler width fluctuations change the mean extinction coefficient as compared to its value (4) taken at the mean Doppler width $\Delta\nu_D^{(0)}$, we average Equation (4) for two realizations. In the first realization, we take $\Delta\nu_D = \Delta\nu_D^{(0)} + \Delta\nu'_D$, and in the second one, $\Delta\nu_D = \Delta\nu_D^{(0)} - \Delta\nu'_D$. The mean value of $\alpha_\nu^{(0)}$ for these two realizations for small value $\Delta\nu'_D/\Delta\nu_D^{(0)} \equiv y$ is equal to

$$\alpha_\nu^{(0)} = \alpha(x)\, e^{-3x^2y^2}\, [(1+y^2)\cosh(2yx^2) - y\sinh(2yx^2)]. \quad (5)$$

Here, we introduce the usual notations

$$\alpha(x) = \frac{\alpha_0}{\Delta\nu_D^{(0)}} \exp(-x^2), \qquad x = \frac{\nu - \nu_0}{\Delta\nu_D^{(0)}}, \quad (6)$$

where $x$ is the dimensionless frequency, and $\alpha(x)$ is the extinction coefficient at the mean Doppler width.

First of all, we see that at the center of the line ($x = 0$) the mean extinction coefficient is greater than the usual extinction factor

$$\alpha_\nu^{(0)} \cong \alpha(0)(1 + y^2), \quad (7)$$

i.e., in the center of the line the stochastic medium is more optically thick compared to the nonstochastic one. For small values ($2yx^2 \ll 1$), we have

$$\alpha_\nu^{(0)} \cong \alpha(x)(1 + y^2 - 5y^2x^2 + 2y^2x^4), \quad (8)$$

i.e., near the center of the line the extinction coefficient $\alpha_\nu^{(0)}$ diminishes and becomes less than the usual $\alpha(x)$-coefficient. Furthermore, we use the normalized extinction factors equal to unity at $x = 0$. The normalized factor is equal to Equation (8) without the term $y^2$. This normalized factor is less than the usual normalized factor $\alpha_{\rm norm}(x) = \exp(-x^2)$ up to $x \cong 1.6$, and then it becomes greater than $\exp(-x^2)$. In the wings of a spectral line, the mean normalized coefficient $\alpha_{\rm norm}^{(0)}(x) \gg \alpha_{\rm norm}(x)$. But, usually, the wings of a spectral line are observed with large errors, and it is difficult to exclude this effect in the pure form. Later, we calculate the $\alpha_\nu^{(0)}$-coefficient exactly using the assumption that the fluctuations $\Delta\nu'_D$ obey the Gaussian distribution function. The presented qualitative picture, drawn above, is confirmed by these exact calculations.

The goal of this paper is to give a simple analytic consideration of how the fluctuations $\Delta\nu'_D$ change the intensity and shape of a spectral line. It will be shown that the distortion of the shape can be fairly large even in the central parts of a line and can be used for the estimation of the levels of fluctuations of the temperature and the local averaged small-scale turbulent velocity in the nonuniform chaotic structure of radiation sources.

Of course, we can estimate only the sum of these fluctuations. But often we have some additional information about their possible values, and in these cases we can obtain very useful restrictions on the levels of fluctuations. In all cases, the simple procedure to describe the observed level of Doppler width fluctuations separately by pure temperature and pure turbulent velocity fluctuations is very useful.

## 3. CALCULATION OF THE MEAN EXTINCTION COEFFICIENT

As is known (see Van Kampen 1981; Rytov et al. 1987), the Gaussian probability function obeys the usual diffusion equation. The evident condition $\Delta\nu_D > 0$ gives rise to the known Green function of the diffusion equation which is equal to zero at $\Delta\nu_D = 0$. So the average value of the extinction factor is calculated from the following expression:

$$\alpha_\nu^{(0)} = \frac{1}{N}\int_0^\infty d(\Delta\nu_D)\left[\exp\left(-\frac{(\Delta\nu_D - \Delta\nu_D^{(0)})^2}{2\langle(\Delta\nu'_D)^2\rangle}\right) - \exp\left(-\frac{(\Delta\nu_D + \Delta\nu_D^{(0)})^2}{2\langle(\Delta\nu'_D)^2\rangle}\right)\right]\frac{\alpha_0}{\Delta\nu_D}\exp\left[-\left(\frac{\nu-\nu_0}{\Delta\nu_D}\right)^2\right], \quad (9)$$

where $N$ is a normalizing constant equal to the integral of the Green function over all values of $\Delta\nu_D$. We calculate this constant numerically for every particular value of the level of fluctuations $\eta$. To calculate the change of the normalized line shape (see below), this constant is not necessary. We see that at $\Delta\nu_D = 0$ the Green function is equal to zero. For small values of the fluctuations (practically, for $\eta < 0.2$–$0.3$), the second term in the Green function can be omitted, and we obtain the usual symmetric Green function for the infinite one-dimensional problem.

Introducing the dimensionless variable $y = (\Delta\nu_D - \Delta\nu_D^{(0)})/\Delta\nu_D^{(0)} \equiv \Delta\nu'_D/\Delta\nu_D^{(0)}$, Equation (9) can be presented in the most simple form

$$\alpha^{(0)}(x,\eta) = \frac{1}{N}\int_{-1}^\infty dy\left[\exp\left(-\frac{y^2}{2\eta^2}\right) - \exp\left(-\frac{(y+2)^2}{2\eta^2}\right)\right] \times \frac{\alpha_0}{\Delta\nu_D^{(0)}(1+y)}\exp\left[-\frac{x^2}{(1+y)^2}\right]. \quad (10)$$

In Figure 1, we present the normalized extinction factor

$$\alpha_{\rm norm}^{(0)}(x,\eta) \equiv \frac{\alpha^{(0)}(x,\eta)}{\alpha^{(0)}(0,\eta)} \quad (11)$$

for various values of parameter $\eta$. A comparison with the usual normalized extinction factor $\alpha_{\rm norm}(x) = \exp(-x^2)$ demonstrates that our qualitative picture, presented above, is really true. The extinction coefficients $\alpha(x)$ and $\alpha^{(0)}(x,\eta)$ are the even functions of the dimensionless frequency $x$, and we present the $\alpha_{\rm norm}^{(0)}(x,\eta)$-factor only for positive $x$.

We see that the normalized extinction factor $\alpha_{\rm norm}^{(0)}(x,\eta)$ for $x < 1.65$ is less than the usual factor $\exp(-x^2)$. Near $x = 1.65$, it becomes greater than $\exp(-x^2)$. For $x = 2.5$ and $\eta = 0.5$, the value $\alpha_{\rm norm}^{(0)}$ is seven times greater than the usual normalized extinction coefficient. Remember that the spectral lines at $x = 2.5$ are practically impossible to observe in the pure form. Besides, for these $x$, the Doppler profile usually does not occur. In the middle of a line, the difference between $\alpha_{\rm norm}^{(0)}(x,\eta)$ and the value $\exp(-x^2)$ is also large.

It is also interesting to compare nonnormalized extinction coefficients $\alpha^{(0)}(x,\eta)$ and $\alpha(x)$. In Table 1, we present the ratio $\alpha^{(0)}(x,\eta)/\alpha(x)$ for a number of values of $x$ and $\eta$. It is seen that this ratio, taken at $x = 0$, monotonically grows with the increase of parameter $\eta$ (we calculated the results only for $\eta \leqslant 0.5$). This means that in the center of a line the stochastic atmosphere is more optically thick than the medium without fluctuations. The inequality $\alpha^{(0)}(x,\eta) > \alpha(x)$ takes place up to $x \simeq 0.45$ for $\eta = 0.1$ and up to $x \simeq 0.25$ for $\eta = 0.5$. For intermediate values of fluctuations, this inequality takes place inside this interval.

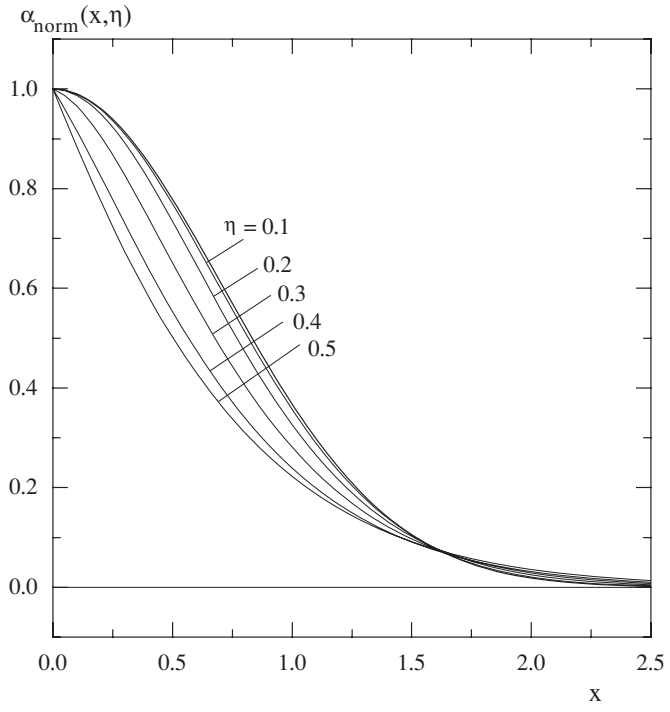


**Figure 1.** Values of the normalized mean extinction coefficient $\alpha^{(0)}_{\rm norm}(x, \eta)$. The bold line presents $\alpha_{\rm norm}(x) = e^{-x^2}$ in the absence of the Doppler width fluctuations ($\eta = 0$). The numbers denote the values of the level of fluctuations $\eta$.

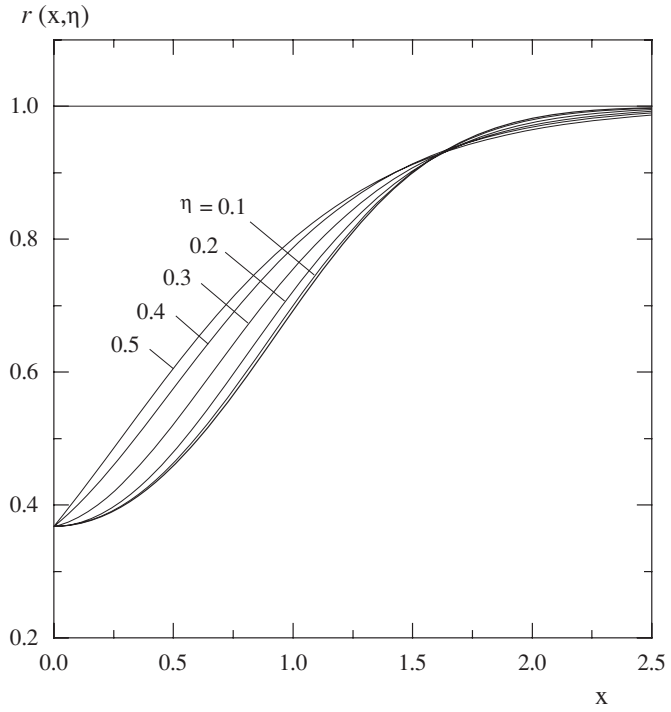


**Figure 2.** Normalized profile of the absorption line at $\tau_0 = 1$. The bold line corresponds to the absence of the Doppler width fluctuations ($\eta = 0$). The numbers denote the values of the level of fluctuations $\eta$.

**Table 1**
Values of $\alpha^{(0)}(x, \eta) / \alpha(x)$

| $\eta$ | 0 | 0.1 | 0.2 | 0.3 | 0.4 | 0.5 |
|---|---|---|---|---|---|---|
| $x = 0$ | 1 | 1.010 | 1.046 | 1.137 | 1.270 | 1.340 |
| 0.25 | 1 | 1.007 | 1.028 | 1.050 | 1.050 | 1.032 |
| 0.5 | 1 | 0.998 | 0.987 | 0.951 | 0.902 | 0.864 |
| 0.75 | 1 | 0.988 | 0.947 | 0.885 | 0.828 | 0.795 |
| 1 | 1 | 0.980 | 0.928 | 0.869 | 0.826 | 0.810 |
| 1.5 | 1 | 1.001 | 1.014 | 1.044 | 1.092 | 1.163 |
| 2 | 1 | 1.126 | 1.421 | 1.786 | 2.180 | 2.617 |

Then the weak opposite inequality takes place, up to $x \approx 1.6$. For $x > 1.6$, the inequality $\alpha^{(0)}(x, \eta) > \alpha(x)$ returns once more, and it becomes stronger with the increase of frequency $x$. This is a purely statistical effect.

## 4. PROPAGATION OF CONTINUUM RADIATION THROUGH A STOCHASTIC SLAB WITH ZERO EMISSIVITY

Here, we consider a simple problem when continuum radiation from a star during its propagation in the interstellar medium meets a slab $L$ of resonant stochastic medium with optical depth $\tau_0 = \alpha^{(0)}(0, \eta)\, L$ in the center of the resonant absorption coefficient. Considering the propagation of continuum radiation in this medium, we can take the intensity of the incident radiation equal to a constant value $I_0$ inside the frequency interval of an absorption line that arises in this case.

The intensities of light in a continuum $I_c$, and in a spectral line frequency range $I_\nu(x, \eta)$ after propagation, through the layer $L$ are

$$I_c = I_0\, e^{-\tau_c},$$
$$I_\nu(x, \eta) = I_0\, e^{-(\tau_c + \tau_0\, \alpha^{(0)}_{\rm norm}(x, \eta))}. \quad (12)$$

The shape of the resulting absorption line is described by the ratio

$$r(x, \eta) = \frac{I_\nu(x, \eta)}{I_c} = e^{-\tau_0 \alpha^{(0)}_{\rm norm}(x, \eta)}. \quad (13)$$

In Figure 2, we present the function $r(x, \eta)$ for the case $\tau_0 = 1$ at the levels of fluctuations $\eta = 0, 0.1, 0.2, 0.3, 0.4$, and 0.5. We see that the fluctuations of the Doppler width give rise to the decrease of the line width compared to the usual layer without the fluctuations ($\eta = 0$). But in the line wings ($x > 1.60$) the situation is opposite—the absorption line becomes larger with the increase of the fluctuations. Remember that in reality, the wings are not described by the Doppler width approximation accepted in our paper. So our analysis is valid only in central parts of a spectral line.

## 5. DISTORTION OF THE ABSORPTION LINE IN A STOCHASTIC PHOTOSPHERE

The origin of the absorption lines in stars' photospheres is more complex than that in the separate layer considered above. A detailed description of this problem is presented in the literature (e.g., Jefferies 1968; Athay 1972; Gray 1992; Kogure & Leung 2007).

To calculate the absorption line profile, we should know the distribution of the radiative source function $S_\nu$, the extinction coefficients of the continuum radiation $\alpha_c$, and the spectral line radiation $\alpha_\nu$ inside the photosphere of a star. In models of photospheres, one uses some mean optical depth $\tau_m$ ($d\tau_m = \alpha_m\, dz$). Usually, the mean extinction coefficient $\alpha_m$ is the Rosseland mean value. The model is known if all physical quantities (e.g., temperature, chemical abundance, the source function $S_\nu$, the extinction factors) are known as functions of $\tau_m$.

The optical depths $\tau_\nu(\tau_m)$ and $\tau_c(\tau_m)$ are equal to

$$\tau_\nu(\tau_m) = \int_0^{\tau_m} d\tau_m' \frac{\alpha_\nu(\tau_m') + \tau_c(\tau_m')}{\alpha_m},$$
$$\tau_c(\tau_m) = \int_0^{\tau_m} d\tau_m' \frac{\alpha_c(\tau_m')}{\alpha_m}. \quad (14)$$

The intensities of the outgoing spectral line and continuum radiation are calculated as follows:

$$I_\nu(\vartheta) = \int_0^\infty \frac{d\tau_m}{\cos\vartheta} S_\nu(\tau_m) e^{-\tau_\nu(\tau_m)/\cos\vartheta}, \quad (15)$$

$$I_c(\vartheta) = \int_0^\infty \frac{d\tau_m}{\cos\vartheta} S_\nu(\tau_m) e^{-\tau_c(\tau_m)/\cos\vartheta}. \quad (16)$$

Here, $\vartheta$ is the angle between the normal to the photosphere and the line of sight **n** directed to an observer. For all stars (besides the Sun), we observe the radiation fluxes $F_\nu$ and $F_c$. So the observed profile of a spectral line is characterized by the expression

$$r_\nu = \frac{F_\nu}{F_c} = \frac{\int_0^\infty d\tau_m\, S_\nu(\tau_m) E_2(\tau_\nu)}{\int_0^\infty d\tau_m\, S_\nu(\tau_m) E_2(\tau_c)}, \quad (17)$$

where the function $E_2(\tau_\nu)$ is determined by the expression

$$E_2(\tau_\nu) = \int_1^\infty \frac{dx}{x^2} e^{-x\,\tau_\nu}. \quad (18)$$

In the early years of absorption line theory, there were some simple approaches for obtaining the formulae for the spectral profile function $r_\nu = F_\nu/F_c$. Most of these approaches considered that the source function $S_\nu(\tau_m)$ coincides with the Planck function $B_\nu(T(\tau_m))$ which, near the star surface, can be represented as linearly depending on the optical depth $\tau_m$ ($B_\nu(\tau_m) \approx B_0(1 + \beta_\nu\tau_m)$). Likewise, one assumes that the ratios $\alpha_\nu/\alpha_m$ and $\alpha_c/\alpha_m$ do not depend on $\tau_m$. These assumptions give rise to the simple formula (Sobolev 1969)

$$r_\nu = \frac{1 + \frac{2}{3}\beta_\nu\alpha_m/(\alpha_\nu + \alpha_c)}{1 + \frac{2}{3}\beta_\nu\alpha_m/\alpha_c},$$
$$\beta_\nu = \frac{3}{8}\frac{h\nu}{kT_0}\frac{1}{1 - e^{-\frac{h\nu}{kT_0}}}. \quad (19)$$

Here, $T_0$ is the temperature at $\tau_m = 0$.

Note that in Rayleigh–Jeans limit ($h\nu/kT_0 \ll 1$), the value $\beta_\nu = 3/8$ is independent of $T_0$ and $\nu$. This means that the large-scale value $\beta_\nu$ (the mean temperature gradient) is less sensitive to small-scale fluctuations than the extinction factor $\alpha_\nu$, which has a local sense. For this reason, one may assume that the mean large-scale radiative source function $S_\nu$ is also practically insensitive to these fluctuations in the photosphere. It seems that the stochasticity of such large-scale functions $S_\nu$ is not correlated with the small-scale fluctuations of the Doppler widths, and it can be averaged independently of the latter.

For weak lines ($\alpha_\nu \ll \alpha_c$) the LTE assumption (without additional suppositions) gives rise to the simple formula (Gray 1992)

$$(1 - r_\nu) \propto \alpha_\nu/\alpha_c. \quad (20)$$

For stochastic photospheres we can use $\alpha^{(0)}(x, \eta)$ instead of $\alpha_\nu$. Besides, we have to use the independently averaged large-scale values $S_\nu$ and $\beta_\nu$ in Equations (17) and (19). Below we use the assumption that these averaged values differ only slightly from those in nonfluctuating photospheres (remember that $\beta_\nu$ in the Rayleigh–Jeans limit is independent of temperature). Strictly speaking, we have to construct the photosphere models using the radiative transfer equation with the averaged extinction factor $\alpha_\nu^{(0)}$ instead of the usual $\alpha_\nu$-factor.

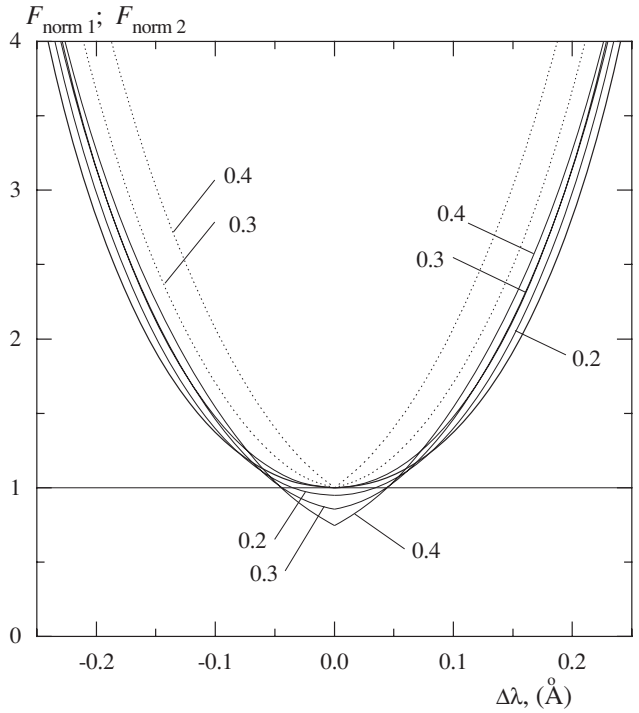


**Figure 3.** Distortion of an absorption spectral line in a stochastic stellar photosphere ($T_{\rm eff} = 10^4$ K, log g = 4, $\lambda_0 = 4475$ Å). The bold curve presents the spectral line $F_{\rm norm\,1}(\Delta\lambda,\ 0) = F_\nu(\Delta\lambda)/F_\nu(0)$ in a nonstochastic photosphere. Dotted lines present values $F_{\rm norm\,1}(\Delta\lambda,\ \eta) = F_\nu(\Delta\lambda,\ \eta)/F_\nu(0,\ \eta)$ and other lines present $F_{\rm norm\,2}(\Delta\lambda,\ \eta) = F_\nu(\Delta\lambda,\ \eta)/F_\nu(0,\ 0)$. Numbers denote the degree of temperature fluctuations $\eta$.

The inequality $\alpha^{(0)}(x, \eta) > \alpha(x)$, mentioned in Section 3, means that absorption lines in stochastic photospheres near the center of a line are "deeper" than in usual photospheres. Statistical increase of $\alpha_\nu$ denotes that the absorption line arises at a smaller distance from the surface compared with nonstochastic photospheres, and the line becomes "deeper." Of course, this also follows from approximate Equations (19) and (20), which have a purely qualitative sense. Below we confirm this statement from calculations using a real model of the photosphere, which does not assume linear dependence of the source function on the optical depth $\tau_m$ and takes into account that $\alpha_\nu/\alpha_m$ and $\alpha_c/\alpha_m$ depend also on $\tau_m$. Of course, we use the usual model of nonfluctuating photospheres.

There are many published models of photospheres (see, for example, Mihalas 1965; Strom & Avrett 1965; Kurucz et al. 1974). We chose model 1 from Strom & Avrett (1965) because they directly present the functions $S_\nu$, $\alpha_\nu/\alpha_m$, and $\alpha_c/(\alpha_c + \alpha_\nu)$ for a number of wavelengths as functions of $\tau_m$. Model 1 in this paper corresponds to a photosphere with $T_{\rm eff} = 10^4$ K and log $g = 4$. This LTE model takes into account the opacities of H, $H^-$, $H_2^+$, He I, He II, electron scattering, and Rayleigh scattering. It does not take into account the blanketing effects.

We chose the wavelength $\lambda = 4475$ Å as the wavelength of the line center. It was more exact to calculate the value $F_\nu$, not $F_c$. For this reason we present in Figure 3 the normalized values

$F_\nu(\Delta\lambda)/F_\nu(0)$ for a nonstochastic photosphere (the bold curve) and the analogous values $F_\nu(\Delta\lambda,\eta)/F_\nu(0,\eta)$ for a stochastic photosphere with the level of fluctuations $\eta = 0.3$ and 0.4 (the dotted curves). It is seen that in the stochastic photosphere the spectral line is narrower than in the usual photosphere. To demonstrate that the stochastic photosphere gives rise to "deeper" lines, we also present the values $F_\nu(\Delta\lambda,\eta)/F_\nu(0)$ for $\eta = 0.2$, 0.3, and 0.4. It is seen that in the center of the line the stochastic effects diminish the intensity. For $\eta = 0.3$ and 0.4, the intensities consist of 86% and 74% of the intensity in the nonstochastic case.

Our calculations were made for a pure thermal Doppler velocity. In this case, the absorption line is very narrow $\Delta\lambda_D \approx 1$ Å. Examples of such narrow absorption lines are presented by Athay (1961).

It should be noted that for the past few decades 2D and 3D nonstationary pure numerical models of stellar atmospheres have been developing (see, e.g., Fraytag & Salaris 1999; Asplund et al. 2000, 2004; Nordlund & Stein 2001; Fraytag et al. 2002; Steffen & Holweger 2002). It seems that in these nonstationary calculations the effects of fluctuations of the Doppler width are included ab initio, as a result of numerical solution of the full system of hydrodynamical and radiative transfer equations. Of course, to obtain the observed mean spectra, the numerical solutions need to be averaged over a large enough time for the calculations (corresponding to many statistical realizations). These hydrodynamical nonstationary theories are very complex and, till now, their general application has been limited (see Ludwig & Kucinskas 2005). The most important achievements of these calculations are the corrections of the chemical element distribution inside the atmospheres.

## 6. PROPAGATION OF A SPECTRAL LINE THROUGH THE STOCHASTIC LAYER

Small distortions in the extinction factor can result in fairly large distortions in observing spectral lines if the incident resonant intensity propagates through an optically thick layer $L$ of matter with fluctuations of temperature and mean small-scale turbulent velocity. The layer can consist of some "sublayers" with different temperature and turbulent velocities, i.e., it can be very inhomogeneous. These distortion effects can be observed most readily in the propagation of maser emission. Maser observations show (see the following section) that most frequently a maser emission line has a Gaussian shape with Doppler width $\Delta\nu_S$. In this case, we obtain the following expression for the observed mean intensity:

$$I^{(0)}(x,\eta) = I_0 e^{-a^2x^2}\, e^{-\tau_0 \underline{\alpha}^{(0)}(x,\eta)}. \tag{21}$$

Here, $x$ is the dimensionless frequency (see Equation (6)) which uses the mean Doppler width $\Delta\nu_D^{(0)}$ corresponding to the layer, parameter $a = \Delta\nu_D^{(0)}/\Delta\nu_S$, and $\tau_0 = \alpha_0/\Delta\nu_D^{(0)}\, L$ is the optical thickness of the layer corresponding to the center of the line for the medium without the fluctuations ($\eta = 0$) (see Equations (6) and (10)). To use this dimensionless parameter we pick out the factor $\alpha_0/\Delta\nu_D^{(0)} \equiv \alpha(0)$ from Equation (10)

$$\alpha^{(0)}(x,\eta) = \frac{\alpha_0}{\Delta\nu_D^{(0)}}\, \underline{\alpha}^{(0)}(x,\eta), \tag{22}$$

where the dimensionless value $\underline{\alpha}^{(0)}(x,\eta)$ describes the extinction coefficient $\alpha^{(0)}(x,\eta)$ in terms of the usual extinction factor $\alpha(0)$, taken in the center of a line. It does not coincide with $\alpha_{\rm norm}(x,\eta)$.

The sense of parameter $a$ is simple. Thus, the case $a = 0.5$ corresponds to the wide incident spectral line, and $a = 2$ corresponds to the narrow incident line as compared to the Doppler width of resonant atoms in the layer. The term $I_0 \exp(-a^2x^2)$ is the incident maser intensity from the source.

In Figure 4, we present normalized intensities $I^{(0)}(x,\eta)/I^{(0)}_{\rm max}$ for various values of the parameters $\tau_0$ and $a$. First of all, we see that the stochastic fluctuations of the Doppler width make the lines slightly narrower than in the nonstochastic medium. But the main distortion occurs near the center of a line, namely, the stochastic fluctuations make the central minimum more profound compared to the nonstochastic medium. It seems this difference can be used for estimation of the parameters $\eta$ and $\tau_0$.

It is interesting to compare our Figure 4 with the analogous Figure 8 of Silant'ev et al. (2006) devoted to the distortions due to the existence of finite-correlated turbulence in the layer. The main difference between these figures is that the finite-correlated turbulence decreases the minimum in the center of a line, in contrast to our case of stochastic Doppler width. Besides, the narrowness of the disturbed lines is greater than in the present case. Remember that the effects of finite-correlated turbulence occur if the mean turbulent velocity $u_{\rm turb}$ is greater than the thermal velocity $u_{th}$. If there are many turbulent cells inside the layer, then the effects of finite-correlated turbulence disappear in all cases. Remember that our effect occurs for small-scale turbulence. To some extent these two types of stochastic effects are complementary to each other.

## 7. MASER EMISSION FROM AN INVERTED STOCHASTIC MEDIUM

A maser emission line arises in an inverted medium where the optical depth of the propagating flux can be considered as a negative value (see Rybicki & Lightman 1979). We use the normalized expression $I_{\rm norm}(x,\eta) = I(x,\eta)/I(0,\eta)$ to investigate the shape of the maser emission line

$$I_{\rm norm}(x,\eta) = \exp\left[\tau_0\left(\alpha^{(0)}_{\rm norm}(x,\eta) - 1\right)\right]. \tag{23}$$

Here, $\tau_0 > 0$ is the magnitude of optical length in the center of the line ($x = 0$), and the definition of $\alpha^{(0)}_{\rm norm}(x,\eta)$ is given in Equation (11). Usually, in cosmic maser sources we have $\tau_0 \gg 1$. For a medium without fluctuations the dimensionless coefficient $\alpha^{(0)}_{\rm norm}(x)$ is equal to $\exp(-x^2)$, and Equation (23) acquires the usual form

$$I_{\rm norm}(x) = \exp\left[\tau_0\left(e^{-x^2} - 1\right)\right]. \tag{24}$$

This expression at small dimensionless frequencies acquires the Gaussian form

$$I_{\rm norm}(x) \simeq \exp\left(-\tau_0\, x^2\right). \tag{25}$$

It is interesting that for $\tau_0 \gg 1$ the exact Equation (24) can also be satisfactorily approximated by the Gaussian curve (25) (see, for example, Strelnitskij 1982) for $x$ inside all the profiles. Indeed, the value $A_1 = I_{\rm norm}(x_1)$ occurs at

$$x_1^2 = \ln\left(1 + \frac{\ln(A_1)}{\tau_0}\right) \to \frac{|\ln(A_1)|}{\tau_0}. \tag{26}$$

For the Gaussian curve (25), we have

$$x_1^2 = \frac{|\ln(A_1)|}{\tau_0}. \tag{27}$$

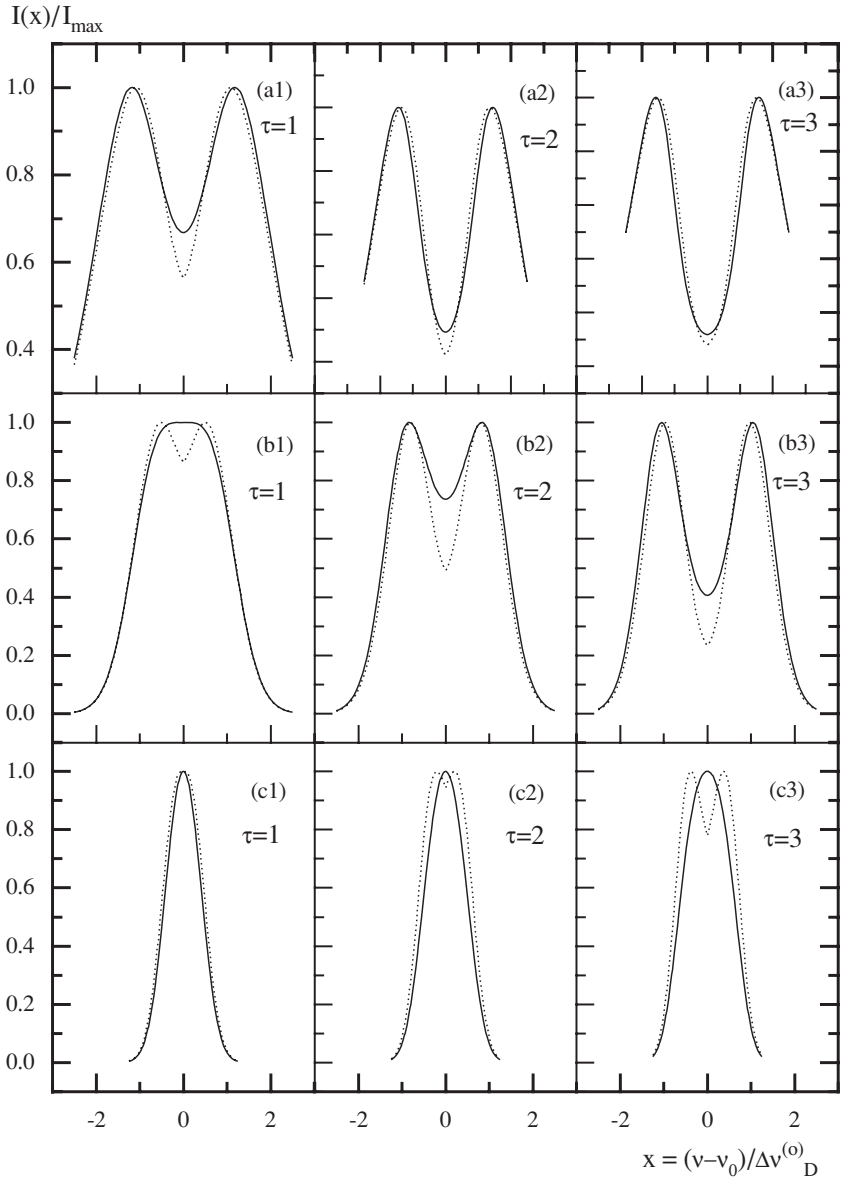


**Figure 4.** Normalized shape $I(x, \tau)/I_{\max}$ of the maser line with a Gaussian initial profile after passage through the layer with the level of fluctuations of stochastic Doppler width $\eta = 0.3$. The bold lines correspond to the usual layer without fluctuations. The cases (a*n*), (b*n*), and (c*n*), with $n = 1, 2, 3 \ldots$, represent cases $a = \Delta\nu_D^{(0)}/\Delta_S = 0.5$, 1, and 2, respectively; $\Delta\nu_D^{(0)}$ and $\Delta\nu_S$ are the Doppler widths in the layer and a maser source. The optical depth of the layer $\tau$ at the line center takes the values 1, 2, and 3.

Equations (26) and (27) coincide with each other for large $\tau_0$, when the inequality $|\ln(A_1)|/\tau_0 \ll 1$ holds. So in the middle of a profile ($A_1 = 0.5$) the $x_1$ values are equal to 0.2680 and 0.2632 at $\tau_0 = 10$ according to Equations (24) and (25), correspondingly. From Equations (26) and (27), one follows that the line width for $\tau_0 \gg 1$ is proportional to $1/\sqrt{\tau_0}$ (see Strelnitskij 1982). Remember that we consider only nonsaturated masers. Of course, saturated masers are observed very frequently.

For these reasons, maser lines are approximated by the Gaussian curve (25). In many observed maser spectra, the Gaussian approximation is very satisfactory. In Figure 5, we present some examples of $H_2O$ maser spectra which practically coincide with the Gaussian curves.

The important problems for maser emission sources are how to estimate the parameters $\tau_0$ and $\Delta\nu_D$. The extremely large maser intensities only denote that $\tau_0 \gg 1$. Maser spectra (see Figure 5) usually refer to radial velocity $u$ connecting with the frequency by the relation $\nu = u\nu_0/c$. It means that the dimensionless frequency $x$ is connected with the radial velocity $u$ by the relation $x = Cu$ with $C = \sqrt{3}/\sqrt{2}u_D$. So the transformation from observed spectra to spectra as functions of dimensionless frequency $x$ is related to knowledge of the effective Doppler velocity $u_D = \sqrt{u_{th}^2 + u_{\rm turb}^2}$ that determines the Doppler width $\Delta\nu_D$ (see Equation (1)).

Formally, we can calculate the values of $\tau_0$ and $u_D$ from the exact Equation (24) using the observable spectra as a function of $u = x/C$. Taking the values $A_1 = I_{\rm norm}(u_1)$ and $A_2 = I_{\rm norm}(u_2)$ from the observed spectrum at $u$—points $u_1$ and $u_2 = \sqrt{2}u_1$—we easily obtain

$$\tau_0 = \frac{\ln(A_1)}{Z - 1}, \qquad u_D = \frac{\sqrt{3}}{\sqrt{2}} \frac{u_1}{\sqrt{|\ln(Z)|}}, \tag{28}$$

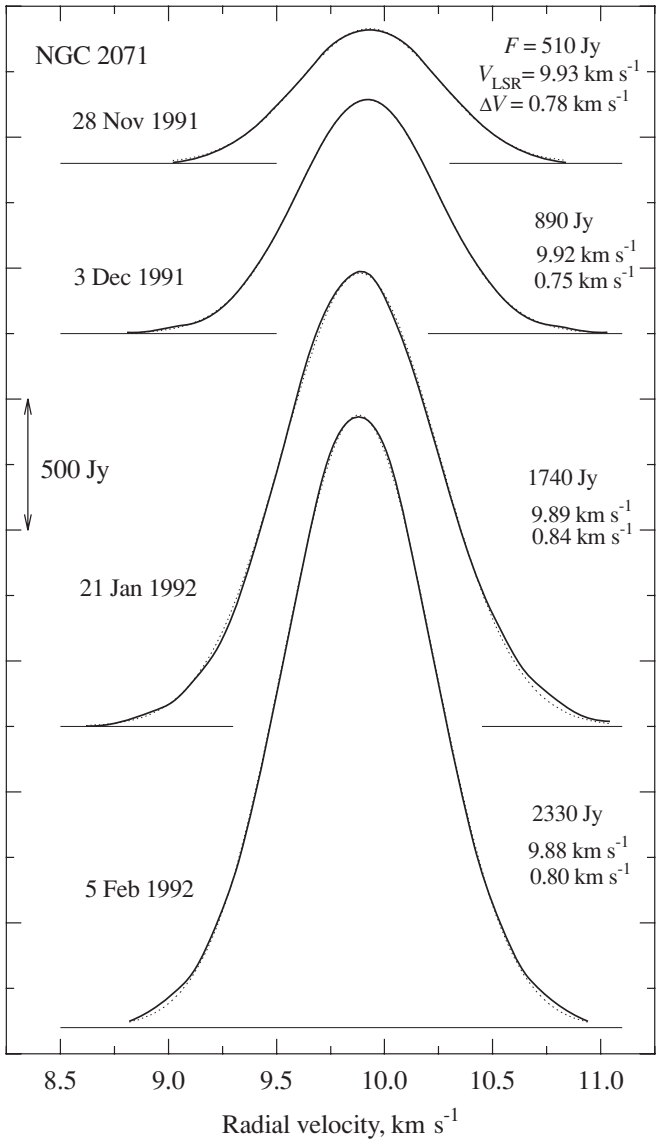


**Figure 5.** Typical flare of $H_2O$ maser emission in NGC2071. At all the stages of the evolution, the radial velocity and the line width change slightly, and the line profile is approximated by the Gaussian curve very satisfactorily (the dotted lines).

where the auxiliary value $Z$ is equal to

$$Z = \frac{\ln(A_2)}{\ln(A_1)} - 1. \quad (29)$$

Unfortunately, for most maser spectra this procedure is practically useless because the spectra have Gaussian form, i.e., they depend on the one parameter $\tau_0 C^2$, not on two separate parameters $\tau_0$ and $C$. We can obtain from Equation (24) the only relation $\tau_0 C^2 = \ln(A_1)/u_1^2$. Equation (28) can be used for masers with $\tau_0 \leqslant 5$. The formula for $\tau_0$ in Equation (28) has logarithmic dependence on values $I_{\rm norm}(x)$, i.e., it is not strongly sensitive to variations of $I_{\rm norm}(x)$. Practically, this means that even for $\tau_0 < 5$ we can estimate the $\tau_0$ value with fairly large errors. The relative insensitivity of the line shape to the value $\tau_0$ also denotes that masers with very different intensities can have practically the same line shapes. The same conclusion is true also for determination of the values $\tau_0\, C^2$ and $u_D$.

## 8. APPLICATION TO THE OBSERVED NON-GAUSSIAN MASER SPECTRA

Most suitable for the investigation of the distortion effects in the spectral lines are the radio lines at $\lambda = 1.35$ cm from $H_2O$ maser sources. According to Varshalovich et al. (2006), the extinction coefficient of $H_2O$ maser radiation has a Gaussian shape at different temperatures—from 200 K up to 900 K—that determines the Doppler width of the spectral line (with the inclusion of small-scale turbulence). The fluctuations of temperature and small-scale turbulent velocities in a maser "spot" tend to the distortion of the Gaussian shape of a line. As a rule, the spectrum of such a source consists of a large number of separate emission features. Every feature is radiating from a separate maser "spot" with dimension $\approx$ 0.1–0.2 AU. Even current interferometers with maximal baselines cannot resolve these spot structures. Here we attempt, using our theory and the observational data, to obtain some estimations concerning the "spot's" parameters, $\tau_0, \eta, u_D$, possible variations of the temperature $T$, and the mean small-scale turbulent velocity $u_{\rm turb}$.

To find a suitable line shape, we analyzed a large number of $H_2O$ maser spectra. These spectra were obtained from long-term monitoring of sources of maser emission in star-formation regions. The monitoring was carried out with the RT-22 radio telescope of the Pushchino Radio Astronomy Observatory (Russia) (see, for example, Berulis & Lekht 1996; Lekht 2000). We took separate emission features, as a rule, during strong flares. In these cases, most of the components are single, and their blending with other lines can be essential only in the wings. We took lines whose blending, if it existed at all, was not higher than the level 0.1–0.15. We chose symmetric lines. This is an additional argument that the line is single. The proof of the line shape was made by the Gaussian fit.

In Figure 5, we present the evolution of an $H_2O$ maser flare in the source NGC2071, that took place in 1991–1992 at a radial velocity of about 9.9 km s$^{-1}$. The dates of observations are given on the left. The fluxes, radial velocities, and line widths are given on the right. The dotted lines show the Gaussian fits. This figure demonstrates that the radial velocity, line width and shape (Gaussian) do not change in spite of large flux variations. It seems the maser is near the saturated regime. This character of the maser emission confirms that the observed feature is single, and that our criteria for the single line choice are correct.

It turns out that symmetric lines with non-Gaussian shape are not frequent. In this paper, we present only those spectra where the non-Gaussian shape is fairly large. We normalized fluxes and the centers of the lines were displaced to zero velocity. For additional safety, we averaged the left and right wings (due to their symmetry) relative to the center of the lines. The resulting spectra for the sources G43.8-0.1, W44C, and W75S are presented in Figures 6–8. The dotted lines show the Gaussian fits. On the left the names, the dates of observations, the radial velocities, and the line widths at the level 0.5 are given.

Now, we remark on the reliability of the observed non-Gaussian line shapes. The observed curves correspond to high level fluxes of maser emission. The possible declinations of points from a smooth curve are determined by the level of noise temperature of the receptor and antenna. In all cases, the relative declinations of line points do not exceed the values 0.3%–1%, whereas the differences between observed line

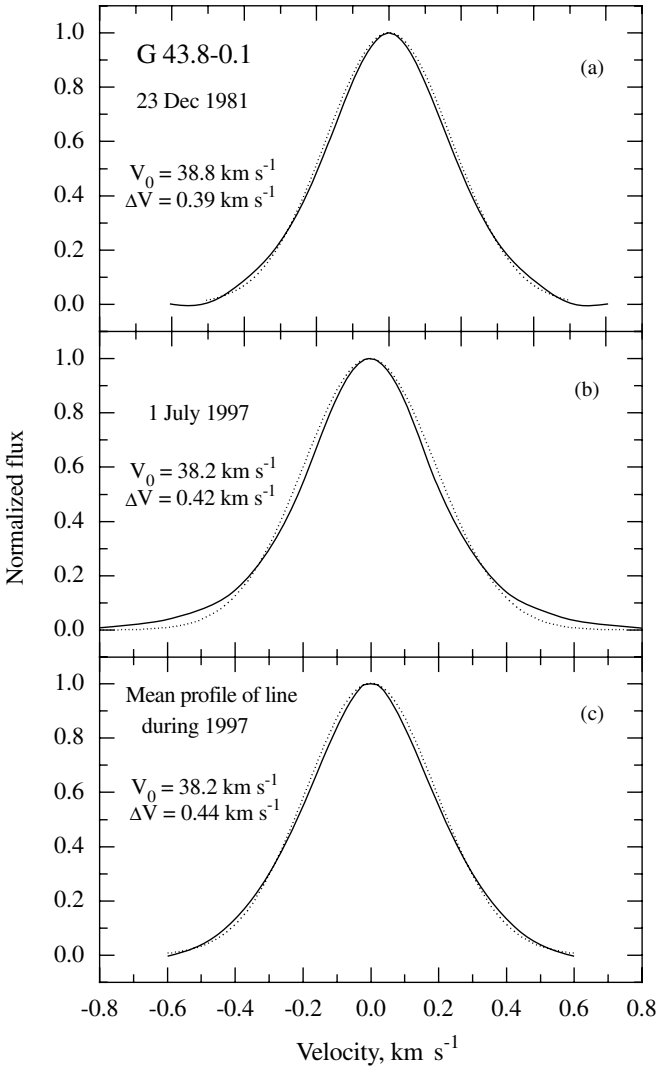


**Figure 6.** Observed $H_2O$ maser line in G43.8-0.1 with non-Gaussian shape. The dotted lines present the approximation by the Gaussian curve.

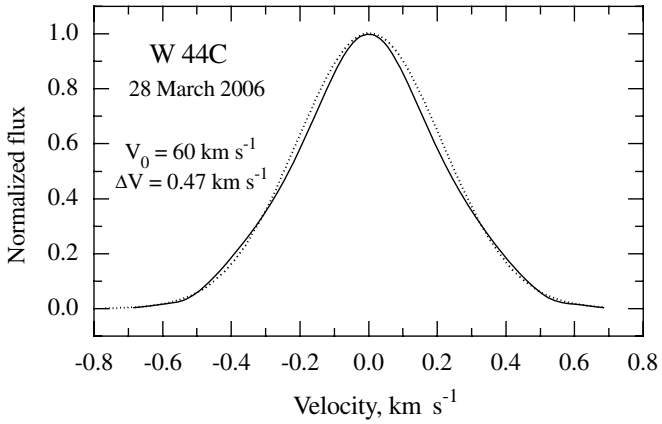


**Figure 7.** Same as in Figure 6 for the source W44C.

shapes and Gaussian fits amount to 5%–8%. Without doubt, the non-Gaussian shape lines were really observed.

Calculation of $I_{\rm norm}(x, \eta)$ (see Equation (23)) for various values of $\tau_0$ and $\eta$, and comparison with the normalized spectra from Figure 6(a)–(c) allow us to estimate the parameters $\tau_0$, $\eta$, $C$, and $u_D$. We found that this estimation is fairly sensitive to the

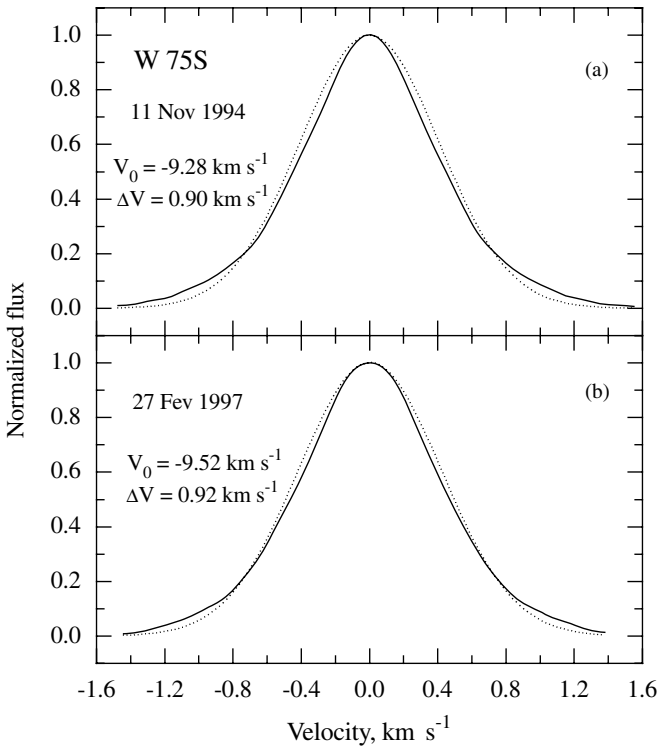


**Figure 8.** Same as in Figure 6 for the source W75S.

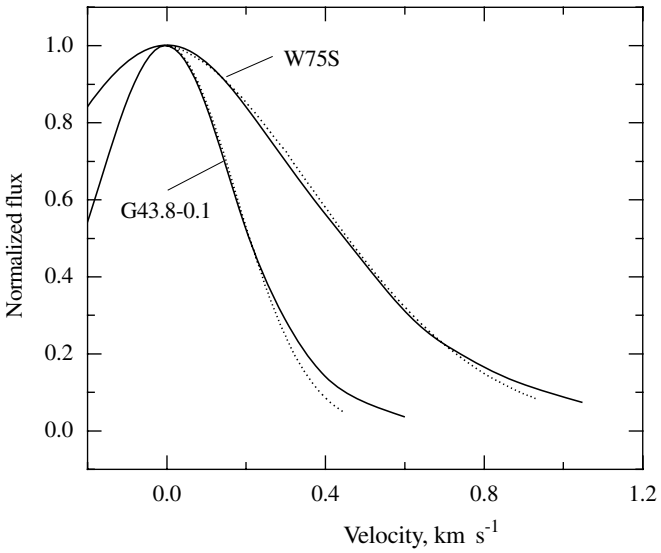


**Figure 9.** Result of approximations of spectra in W75S and G43.8-0.1. The bold curves present the observed spectra, and the dotted lines present their approximation by Equation (23). The parameters used are given in Table 2.

choice of the parameter $\eta$. Practically, we can distinguish the cases $\eta \pm 0.02$. The dependence of Equation (23) on $\tau_0$ is not so strong compared to the case of Equation (24). The reason is pointed out below. Because the deviation of the line shape from the Gaussian form is usually low, our explanation is also valid for the case of lines with non-Gaussian shape. Nevertheless, the non-Gaussian case gives an additional chance to estimate the values $\tau_0$ and $u_D$ separately, especially for large deviations from the Gaussian shape.

In Figure 9, we present the results of the approximation by Equation (23) of the observed non-Gaussian spectra in the sources W75S and G43.8-0.1. In these cases, the deviations

**Table 2**
Values of Basic Parameters of Various $H_2O$ Maser Features Having Non-Gaussian Line Shape

| Source | Date | $\tau_0$ | $\eta$ | $u_D$, km s$^{-1}$ | $C$ |
|---|---|---|---|---|---|
| W75S | 1994 Nov 11 | 26 | 0.25 | 4.6 | 0.27 |
| W44C | 2006 Mar 28 | 31 | 0.26 | 2.8 | 0.43 |
| G43.8-0.1 | 1981 Dec 23 | 33 | 0.25 | 0.54 | 2.3 |
| | 1997 Jul 1 | 32 | 0.15 | 0.68 | 1.8 |
| | 1997 | 31 | 0.25 | 2.4 | 0.50 |

from the Gaussian shape are fairly large (see Figures 6 and 8). In Table 2, we present the results of approximations by Equation (23) for a number of non-Gaussian spectra. We practically exactly approximated the spectra in three different points of a spectrum. This diminishes considerably the possible variants for the choice $\tau_0$. It seems the possible deviation of this parameter is $\Delta\tau_0 = \pm 2$. The same relative error has the determination of the constant $C$, and connected with it is the mean effective Doppler velocity $u_D^{(0)} = \sqrt{1.5}/C$.

We see that the level of the Doppler width fluctuations $\eta$ (see Equation (3)) in all these sources is fairly large $\eta \simeq 0.15$–$0.25$. It means that in these sources there are large fluctuations of the temperature $T$ and the mean turbulent velocities $u_{\rm turb}$. The obtained values of mean effective Doppler velocity are also rather large (see Table 2), and demonstrate that the turbulent velocities give the main contribution to $u_D^{(0)}$. So if we take the maximum mean temperature in the sources equal to 625 K ($u_{th} \simeq 0.92$ km s$^{-1}$) (see, for example, Varshalovich et al. 2006), then the required turbulent velocity is $u_{\rm turb} \gg u_{th}$.

## 9. SUMMARY

Stochastic variations of temperature $T$ and mean turbulent velocity $u_{\rm turb}$ determine the corresponding stochastic variations of the Doppler width $\Delta\nu_D$ of a spectral line. We observe the mean intensities $I_\nu^{(0)}$ from the stochastic atmospheres of stars and interstellar media. These intensities are described by the mean values of the extinction coefficient $\alpha_\nu^{(0)}$ that differs fairly strongly from the usual extinction factor $\alpha(x) = \alpha(0)\exp(-x^2)$ (here $x = (\nu - \nu_0)/\Delta\nu_D$ is dimensionless frequency).

We have calculated the mean extinction coefficient assuming a Gaussian probability distribution of the Doppler width fluctuations. The value $\alpha_\nu^{(0)}$ in the center of the line ($x = 0$) is always greater than the usual coefficient $\alpha(0)$. This means that near the center of a spectral line a stochastic medium is less transparent than a nonstochastic one. At some distance $x$ from the center of a line, the value of $\alpha_\nu^{(0)}$ is lower than $\alpha(x)$, and for $x > 1.60$–$1.65$, in the wing of a line, the value $\alpha_\nu^{(0)} \gg \alpha(x)$. Such a complex form of the mean extinction factor gives rise to distortions of the observed spectral line shape.

First, the absorption lines in stochastic media are narrower than in nonstochastic ones in the central parts of a line ($x < 1.6$), and are wider in the wings. The propagation of a spectral line through the stochastic layer of a gas shows more profound minima in the center of the line compared to the nonstochastic medium. The absorption line acquires a non-Gaussian shape.

Stochastic media with an inverted distribution of atoms and molecules give rise also to the non-Gaussian shape of the outgoing maser radiation. This feature allows us, in principle, to estimate the optical length at the center of the line $\tau_0$ and the effective mean Doppler velocity $u_D^{(0)}$, connected with the mean thermal and turbulent velocities. Remember that from the Gaussian shape one can estimate only the ratio $\tau_0/\left(u_D^{(0)}\right)^2$.

We have observed $H_2O$ maser lines with non-Gaussian shape in a number of sources (e.g., W75S, G43.8-0.1). The approximation of some of them (having the most profound non-Gaussian shape) with the theoretical shape allows us to estimate the values $\tau_0$, $u_D^{(0)}$, and the level of the Doppler fluctuations $\eta \simeq 0.15$–$0.25$. The calculated value of the effective Doppler velocity demonstrates that in these sources the small-scale turbulent velocities are larger than the thermal ones. It means that the stochastic fluctuations of $\Delta\nu_D$ are mainly due to fluctuations in the mean turbulent velocities. This seems quite reasonable for these variable sources in regions of stellar formation.

Maser emission lines with non-Gaussian shape are not frequent during the observations, but they can serve as an additional method for the investigation of the physical parameters in maser "spots." Of course, the distortions of the absorption lines can also be useful for estimating the physical parameters in atmospheres.

The authors are grateful to an anonymous referee for numerous remarks which helped considerably improve the manuscript.

## REFERENCES

Asplund, M., Ludwig, H.-G., Nordlund, A., & Stein, R. F. 2000, A&A, 369, 681
Asplund, M., Grevesse, N., Sauval, A. J., Allende Prieto, C., & Kiselman, D. 2004, A&A, 417, 751
Athay, R. G. 1961, ApJ, 134, 765
Athay, R. G. 1972, Radiation Transport in Spectral Lines (Dordrecht: Reidel)
Berulis, I. I., & Lekht, E. E. 1996, Astron. Rep., 40, 36
Fraytag, B., & Salaris, M. 1999, ApJ, 513, L49
Fraytag, B., Steffen, M., & Dorch, B. 2002, Astron. Nachr., 323, 213
Gray, D. F. 1992, The Observation and Analysis of Stellar Photospheres (Cambridge: Cambridge Univ. Press)
Gurzadyan, G. A. 1980, Flare Stars (Oxford: Pergamon)
Hummer, D. G. 1962, MNRAS, 125, 21
Jefferies, J. T. 1968, Spectral Line Formation (Massachusetts, MA: Blaisdell)
Kogure, T, & Leung, K.-C. 2007, The Astrophysics of Emission-Line Stars (New York: Springer)
Kurucz, R. L., Peytremann, E., & Avrett, E. H. 1974, Blanketed Model Atmospheres for Early-Type Stars (Washington, DC: Smithsonian Institution)
Lekht, E. E. 2000, A&A, 141, 185
Levshakov, S. A., & Kegel, W. H. 1997, MNRAS, 288, 787
Ludwig, M., & Kucinskas, A. 2005, ESASP, 566, 319
Mihalas, D. 1965, ApJS, 11, 184
Nordlund, A., & Stein, R. F. 2001, ApJ, 546, 576
Rybicki, G. B., & Lightman, A. P. 1979, Radiative Processes in Astrophysics (New York: Wiley)
Rytov, S. M., Kravtsov, Yu., A., & Tatarskii, V. I. 1987, Principles of Statistical Radiophysics (Berlin: Springer)
Silant'ev, N. A. 2005, A&A, 433, 1117
Silant'ev, N. A., & Alexeeva, G. A. 2008, A&A, 479, 207
Silant'ev, N. A., Lekht, E. E., Mendoza-Torres, J. E., & Rudnitskij, G. M. 2006, A&A, 453, 989
Sobolev, V. V. 1969, Course in Theoretical Astrophysics, National Aeronautic and Space Administration, NASA technical translation, NASA TT F-531
Steffen, M., & Holweger, H. 2002, A&A, 387, 258
Sterken, C., & Jaschek, C. (ed.) 1996, Light Curves of Variable Stars (Cambridge: Cambridge Univ. Press)
Stix, M. 1991, The Sun, An Introduction (Berlin: Springer)
Strelnitskij, V. S. 1982, SvAL, 8, 86
Strom, S. E., & Avrett, E. H. 1965, ApJS, 12, 1
Van Kampen, N. G. 1981, Stochastic Processes in Physics and Chemistry (Amsterdam: North-Holland)
Varshalovich, D. A., Ivanchik, A. V., & Babkovskaya, N. S. 2006, Astr. Lett., 32, 29